

Multiple Time Scales in Classical and Quantum–Classical Molecular Dynamics

Sebastian Reich

Department of Mathematics and Statistics, University of Surrey, Guildford, Surrey GU2 5XH, United Kingdom

E-mail: s.reich@surrey.ac.uk

Received July 6, 1998; revised October 6, 1998

The existence of multiple time scales in molecular dynamics poses interesting and challenging questions from an analytical as well as a numerical point of view. In this paper, we consider simplified models with two essential time scales and describe how these two time scales interact. The discussion focuses on classical molecular dynamics (CMD) with fast bond stretching and bending modes and the so-called quantum–classical molecular dynamics (QCMD) model where the quantum part provides the highly oscillatory solution components. The analytic results on the averaging over fast degrees of motion will also shed new light on the appropriate implementation of multiple-time-stepping algorithms for CMD and QCMD. © 1999 Academic Press

1. INTRODUCTION

Classical molecular dynamics (CMD) [1] leads to Newtonian equations of motion with fast bond stretching and bending modes and a relatively slow motion in the remaining degrees of freedom. For numerical integration, the Verlet method [43] is typically used with a step size that resolves the fast bond stretching/bending modes. However, often one is interested in the computation of slowly varying quantities and/or time averages, and a method such as Verlet can quickly become inefficient for long-time simulations.

Various approaches have been suggested to improve the classical Verlet method. Among these are (i) methods based on the explicit elimination of the fast bond stretching/bending modes and the subsequent integration of the corresponding constrained equations of motion by the SHAKE or RATTLE method [2, 37] and (ii) reversible multiple-time-stepping (MTS) methods [7, 23, 42] that use different time steps for the fast and slow degrees of freedom.

In appropriate (local) coordinates, the fast bond stretching and bending modes can be reduced to weakly coupled harmonic oscillators whose frequency depends on the slow modes. This dependence leads to a coupling of the slow and fast modes, which, in general, implies that the fast degrees of motion cannot be removed from the model without changing

its long-time dynamics [11, 14, 32, 36, 41]. It seems that in those situations only methods based on the idea of MTS can and should be used for enhanced classical molecular dynamics. However, one must be careful: straightforward application of a MTS method may lead to wrong results or to unstable computations [7, 9]. This fact is briefly discussed in Section 2. An improved approach to multiple time stepping has been suggested by García-Archilla *et al.* in [19]. In Section 5, we consider a variant of this approach [26, 34] that is particularly suited for the multiple time scale integration of CMD.

In recent years, the combination of quantum and classical molecular dynamics has become important. In this paper, we focus on the so-called quantum–classical molecular dynamics (QCMD) model [6, 12, 13, 20, 21], where most of the molecular system is described by classical Newtonian equations of motion while a small but important part is modeled by a time-varying Schrödinger equation (see Section 3). Again, the fast quantum degrees of freedom and the slow classical degrees of freedom are tightly coupled. In fact, the effect of this coupling on the (slow) classical degrees of freedom, which is linked to the Born–Oppenheimer approximation [13], is easier to understand than the corresponding coupling effects in classical molecular dynamics. However, as we will show in Section 4, classical molecular dynamics can be transformed to a system resembling the QCMD model, and theoretical results derived for the QCMD model can also be applied to classical molecular dynamics. This is confirmed by the numerical simulation of a simple test problem.

Because of the importance of the QCMD model, we also discuss MTS methods for QCMD [30, 31, 39]. Here it is crucial to observe that the method has to be implemented in an appropriate way and that some of the straightforward implementations can lead to erroneous numerical results in the (slow) classical degrees of freedom [24, 30, 31]. This aspect is discussed in Section 6.

2. CLASSICAL MOLECULAR DYNAMICS AND MULTIPLE TIME STEPPING

The atomic motion of a molecular system, consisting of N atoms, is typically described by Newtonian equations of motion of the form

$$\dot{\mathbf{q}} = \mathbf{M}^{-1}\mathbf{p}, \quad (1)$$

$$\dot{\mathbf{p}} = -\nabla_{\mathbf{q}}\mathcal{V}(\mathbf{q}) - \sum_{i=1}^m \mathbf{G}_i(\mathbf{q})^T k_{ii} g_i(\mathbf{q}), \quad (2)$$

where $\mathbf{q} \in \mathcal{R}^{3N}$ is the vector of all atomic positions, $\mathbf{p} \in \mathcal{R}^{3N}$ the vector of the corresponding momenta, $\mathbf{M} \in \mathcal{R}^{3N \times 3N}$ the diagonal mass matrix, and $\mathcal{V}(\mathbf{q})$ the potential energy except for the terms corresponding to bond stretching and bending which are described by the second term on the left-hand side of Eq. (2). Here the functions $\{g_i\}_{i=1,\dots,m}$ can either stand for $g_i(\mathbf{q}) = r - r_0$ (bond stretching) or $g_i(\mathbf{q}) = \phi - \phi_0$ (bond angle bending). In either case, $\mathbf{G}_i(\mathbf{q}) \in \mathcal{R}^{3N}$ denotes the Jacobian of $g_i(\mathbf{q})$ and k_{ii} the force constant. For compactness of notation, we collect the functions $\{g_i\}$ in the vector-valued function \mathbf{g} , the force constants $\{k_{ii}\}$ in the diagonal matrix $\mathbf{K} \in \mathcal{R}^{m \times m}$, and the Jacobians $\{\mathbf{G}_i(\mathbf{q})\}$ in the matrix $\mathbf{G}(\mathbf{q}) \in \mathcal{R}^{m \times 3N}$. This gives rise to the equations

$$\dot{\mathbf{q}} = \mathbf{M}^{-1}\mathbf{p}, \quad (3)$$

$$\dot{\mathbf{p}} = -\nabla_{\mathbf{q}}\mathcal{V}(\mathbf{q}) - \mathbf{G}(\mathbf{q})^T \mathbf{K}\mathbf{g}(\mathbf{q}). \quad (4)$$

The total energy

$$\mathcal{H} = \frac{1}{2} \mathbf{p}^T \mathbf{M}^{-1} \mathbf{p} + \mathcal{V}(\mathbf{q}) + \frac{1}{2} \mathbf{g}(\mathbf{q})^T \mathbf{K} \mathbf{g}(\mathbf{q})$$

is a conserved quantity (first integral) along solutions of (3)–(4).

Let us denote the potential energy of the system by $U(\mathbf{q})$, i.e.,

$$U(\mathbf{q}) := \mathcal{V}(\mathbf{q}) + \frac{1}{2} \mathbf{g}(\mathbf{q})^T \mathbf{K} \mathbf{g}(\mathbf{q}),$$

and the kinetic energy by $T(\mathbf{p})$. Then the Verlet method [43] can be considered as a composition method [40] based on the exact solution operators of the two systems

$$\begin{aligned} \dot{\mathbf{q}} &= \nabla_{\mathbf{p}} T(\mathbf{p}) = \mathbf{M}^{-1} \mathbf{p}, \\ \dot{\mathbf{p}} &= \mathbf{0} \end{aligned}$$

and

$$\begin{aligned} \dot{\mathbf{q}} &= \mathbf{0}, \\ \dot{\mathbf{p}} &= -\nabla_{\mathbf{q}} U(\mathbf{q}). \end{aligned}$$

Let us denote these solution operators by $\exp(tL_T)$ and $\exp(tL_U)$, respectively. Then one step of the Verlet method with a step size δt is equivalent to the concatenation

$$\exp\left(\frac{\delta t}{2} L_U\right) \cdot \exp(\delta t L_T) \cdot \exp\left(\frac{\delta t}{2} L_U\right).$$

Because each solution operator is volume preserving (and even symplectic), the Verlet method is volume preserving (symplectic) [40]. Furthermore, the method conserves linear and angular momentum and the time reversibility of the Newtonian equations of motion.

The Verlet method becomes inefficient if the evaluation of the force field is expensive due to long-range interactions. To enhance the classical Verlet method, a symplectic and time-reversible MTS method was suggested in [7, 23, 42]. The idea of this MTS method is amazingly simple: We split the total potential energy U into two terms U_1 and U_2 with U_1 containing all the short-range interactions (in particular the bond stretching/bending modes). Then one step of a MTS scheme with macro step size $\Delta t = j\delta t$, $j \gg 1$, reads¹

$$\exp\left(\frac{\Delta t}{2} L_{U_2}\right) \cdot \underbrace{\left[\exp\left(\frac{\delta t}{2} L_{U_1}\right) \cdot \exp(\delta t L_T) \cdot \exp\left(\frac{\delta t}{2} L_{U_1}\right) \right]}_{j \text{ times}} \cdot \exp\left(\frac{\Delta t}{2} L_{U_2}\right). \quad (5)$$

This method has the same conservation properties as the Verlet method, but it is potentially more efficient since the long-range forces have to be computed less frequently.

Although the idea of (5) is simple, the method has some drawbacks. For certain values of the macro step size Δt , the method can become unstable (meaning a systematic increase in

¹ See Fig. 3 in Section 5 for a more explicit formulation of (5).

total energy) due to resonance/sampling phenomena [7, 9]. Even if there is no systematic increase in the total energy, the numerical results can be qualitatively different from those obtained from the standard Verlet method. This effect does not occur for systems with strong bond bending/stretching potentials. But it can be observed for systems with very light particles if the splitting of the Hamiltonian is not done properly. We will also encounter this problem when discussing MTS methods for the QCMD model.

EXAMPLE 1. We take two harmonic oscillators $\mathcal{H}_x = (p_x)^2/2 + (q_x)^2/2$ and $\mathcal{H}_y = (p_y)^2/(2\epsilon^2) + (q_y)^2/2$, one of which has a very small “mass” $m = \epsilon^2$, $\epsilon \rightarrow 0$, coupled by a quadratic potential $\mathcal{W} = q_x q_y$:

$$\mathcal{H} = \frac{1}{2}(p_x)^2 + \frac{\epsilon^{-2}}{2}(p_y)^2 + \frac{1}{2}(q_x)^2 + \frac{1}{2}(q_y)^2 + q_x q_y.$$

The equations of motion are

$$\begin{aligned}\dot{q}_x &= p_x, \\ \dot{p}_x &= -q_x - q_y, \\ \dot{q}_y &= \epsilon^{-2} p_y, \\ \dot{p}_y &= -q_y - q_x.\end{aligned}$$

The last two equations describe a highly oscillatory motion about the “equilibrium” $(-q_x, 0)$. If this solution is used in the second equation to time-average over the rapidly oscillating force term

$$F(t) = -q_x - q_y(t),$$

we obtain the averaged force $\langle F \rangle \approx 0$. Thus, the “slow” dynamics in the variable (q_x, p_x) is approximately given by the equations

$$\begin{aligned}\dot{q}_x &= p_x, \\ \dot{p}_x &= 0.\end{aligned}$$

A MTS scheme can be obtained via the splitting

$$\begin{aligned}T &= \frac{1}{2}(p_x)^2 + \frac{\epsilon^{-2}}{2}(p_y)^2, \\ U_1 &= \frac{1}{2}(q_y)^2,\end{aligned}$$

and

$$U_2 = \frac{1}{2}(q_x)^2 + q_x q_y.$$

We assume that the step size $\delta t < \epsilon$ in (5) is chosen small enough such that the equations of motion corresponding to the Hamiltonian $T + U_1$ are solved “exactly.” Next we define the macro step size Δt such that the solutions to $T + U_1$ satisfy $q_y(\Delta t) \approx q_y(0)$ and

$p_y(\Delta t) \approx p_y(0)$, i.e., $\Delta t \approx k\epsilon/(2\pi)$, $k \gg 1$. Thus, instead of sampling a highly oscillatory solution, we obtain a fictitious “constant” solution which, when plugged into the numerical approximation of

$$\dot{p}_x = -q_x - q_y(t) = F(t),$$

leads, in general, to a qualitatively wrong approximation of the averaged force $\langle F \rangle$. This problem does not occur if the splitting

$$U_1 = \frac{1}{2}(q_y)^2 + q_x q_y$$

and

$$U_2 = \frac{1}{2}(q_x)^2$$

is used.

An alternative to the MTS scheme (5) is to replace the Verlet discretization of $T(\mathbf{p}) + U_1(\mathbf{q})$ in the inner loop of (5) with one step with an implicit method (such as the implicit midpoint rule [40]) and step size $\delta t = \Delta t$. However, in addition to the resonance problems of the MTS method (5) [28], one also, in general, encounters an exponential instability unless the step size Δt is chosen sufficiently small [4]. Thus such an approach seems inappropriate for CMD simulations.

3. QUANTUM–CLASSICAL MOLECULAR DYNAMICS

3.1. The QCMD Model

Various extensions of classical mechanics to also include quantum effects have been introduced in the literature. Here we consider the so-called quantum–classical molecular dynamics model. In the QCMD model (see [6, 12, 13, 20, 21] and references therein), most atoms are described by classical mechanics, but an important small portion of the system is described by quantum mechanics. This leads to a coupled system of Newtonian and Schrödinger equations.

For ease of presentation, we consider the case of just one quantum degree of freedom with spatial coordinate x and mass m and N classical particles with coordinates $\mathbf{q} \in \mathcal{R}^{3N}$ and diagonal mass matrix $\mathbf{M} \in \mathcal{R}^{3N \times 3N}$. Upon denoting the interaction potential by $V(x, \mathbf{q})$, we obtain the following equations of motion for the QCMD model,

$$\begin{aligned} \dot{\psi} &= -\frac{i}{\hbar} H(\mathbf{q})\psi, \\ \dot{\mathbf{q}} &= \mathbf{M}^{-1}\mathbf{p}, \\ \dot{\mathbf{p}} &= -\langle \psi, \nabla_{\mathbf{q}} H(\mathbf{q})\psi \rangle - \nabla_{\mathbf{q}} U(\mathbf{q}), \end{aligned}$$

with $U(\mathbf{q})$ the purely classical potential energy and $H(\mathbf{q})$ the quantum Hamiltonian operator typically given by

$$H(\mathbf{q}) = T + V(x, \mathbf{q}), \quad T = -\frac{\hbar^2}{2m} \Delta_x.$$

In what follows, we assume that the quantum subsystem has been truncated to a finite-dimensional system by an appropriate spatial discretization and a corresponding representation of the wave function ψ by a complex-valued vector $\psi \in \mathcal{C}^d$. The discretized quantum operators T , V , and H are denoted $\mathbf{T} \in \mathcal{C}^{d \times d}$, $\mathbf{V}(\mathbf{q}) \in \mathcal{C}^{d \times d}$, and $\mathbf{H}(\mathbf{q}) \in \mathcal{C}^{d \times d}$, respectively.

The total energy of the system

$$\mathcal{H} = \frac{\mathbf{p}^T \mathbf{M}^{-1} \mathbf{p}}{2} + \langle \psi, \mathbf{H}(\mathbf{q}) \psi \rangle + U(\mathbf{q}) \quad (6)$$

is a conserved quantity of the QCMD model. Here

$$\langle \psi, \mathbf{H}(\mathbf{q}) \psi \rangle := \bar{\psi}^T \mathbf{H}(\mathbf{q}) \psi$$

and $\bar{\psi}$ denotes the complex conjugate of ψ . Another conserved quantity is the norm of the vector ψ , i.e., $\langle \psi, \psi \rangle = \text{const.}$ due to the unitary propagation of the quantum part.

In the context of this paper, an important conservation property of the QCMD model is related to its Hamiltonian structure, which implies the symplecticness of the solution operator [3]. There are different ways to consider the QCMD model as a Hamiltonian system with Hamiltonian (6). Here we basically² follow the presentation given in [12, 38]: We decompose the complex-valued vector ψ into its real and imaginary part, i.e.,

$$\psi = \frac{1}{\sqrt{2}}(\mathbf{q}_\psi + \mathbf{i}\mathbf{p}_\psi). \quad (7)$$

Then, the equations of motion can be derived from the scaled Lie–Poisson bracket

$$\{F, G\} = \hbar^{-1} \{F, G\}_{\mathbf{q}_\psi, \mathbf{p}_\psi} + \{F, G\}_{\mathbf{q}, \mathbf{p}}; \quad (8)$$

i.e.,

$$\dot{f} = \{f, \mathcal{H}\}$$

describes the time evolution of a function f under the Hamiltonian \mathcal{H} . The brackets $\{F, G\}_{\mathbf{q}_\psi, \mathbf{p}_\psi}$ and $\{F, G\}_{\mathbf{q}, \mathbf{p}}$ in (8) stand for the canonical bracket of classical mechanics [3]. For example, $\{F, G\}_{\mathbf{q}, \mathbf{p}} = [\nabla_{\mathbf{q}} F]^T \nabla_{\mathbf{p}} G - [\nabla_{\mathbf{p}} F]^T \nabla_{\mathbf{q}} G$.

3.2. The Limit Behavior of the QCMD Model

It is of interest to consider the limit³ $\hbar \rightarrow 0$ for a fixed energy function (6). As explicitly shown by Bornemann and Schütte in [13, 15] using homogenization techniques, the QCMD model reduces to the Born–Oppenheimer approximation if the symmetric matrix $\mathbf{H}(\mathbf{q})$ can be smoothly diagonalized and its (real) eigenvalues $\{E_i(\mathbf{q}(t))\}_{i=1, \dots, d}$ are pairwise different. This implies that the populations $|\theta_i(t)|^2$, $i = 1, \dots, k$, corresponding to the eigenvalues $E_i(\mathbf{q}(t))$ of the operator $\mathbf{H}(\mathbf{q})$ become adiabatic invariants. Without going through a detailed analysis, this can be seen from the following averaging argument. Let

² We use a different scaling in (7), which leads to the scaled canonical structure (8) of phase space.

³ One should really consider the limit $\mathbf{M} \rightarrow \infty$, i.e., should increase the mass of the classical particles. But this is equivalent, after an appropriate rescaling of time, to taking the limit $\hbar \rightarrow 0$.

we assume that there is a matrix-valued function $\mathbf{Q}(\mathbf{q}) \in \mathcal{R}^{d \times d}$ such that (i) $\mathbf{Q}(\mathbf{q})^T \mathbf{Q}(\mathbf{q}) = \mathbf{I}$ and (ii) $\mathbf{E}(\mathbf{q}) := \mathbf{Q}(\mathbf{q}) \mathbf{H}(\mathbf{q}) \mathbf{Q}(\mathbf{q})^T$ is diagonal. For simplicity, we consider only one classical degree of freedom, i.e., $(\mathbf{q}, \mathbf{p}) = (q, p) \in \mathcal{R}^2$. Next we introduce the new vector

$$\boldsymbol{\theta} := \mathbf{Q}(q) \boldsymbol{\psi} \in \mathcal{C}^d$$

and obtain the transformed QCMD equations of motion

$$\dot{\boldsymbol{\theta}} = -\frac{i}{\hbar} \mathbf{E}(q) \boldsymbol{\theta} + M^{-1} p \mathbf{A}(q) \boldsymbol{\theta}, \quad (9)$$

$$\dot{q} = M^{-1} p, \quad (10)$$

$$\dot{p} = -\langle \boldsymbol{\theta}, \mathbf{Q}(q) \nabla_q \mathbf{H}(q) \mathbf{Q}(q)^T \boldsymbol{\theta} \rangle - \nabla_q U(q) \quad (11)$$

with the skew-symmetric matrix $\mathbf{A}(q) := \nabla_q \mathbf{Q}(q) \mathbf{Q}(q)^T$. Note that $M^{-1} p \mathbf{A}(q) = \dot{\mathbf{Q}}(q) \mathbf{Q}(q)^T$. The fast motion is given by the diagonalized time-dependent Schrödinger equation

$$\dot{\boldsymbol{\theta}} = -\frac{i}{\hbar} \mathbf{E}(q) \boldsymbol{\theta} \quad (12)$$

and the Hellmann–Feynman force F_{HF} [12], acting on the classical particles, can be written as

$$F_{\text{HF}} = -\langle \boldsymbol{\theta}, \mathbf{Q}(q) \nabla_q \mathbf{H}(q) \mathbf{Q}(q)^T \boldsymbol{\theta} \rangle = -\langle \boldsymbol{\theta}, \nabla_q \mathbf{E}(q) \boldsymbol{\theta} \rangle + \langle \boldsymbol{\theta}, [\mathbf{A}(q) \mathbf{E}(q)] \boldsymbol{\theta} \rangle, \quad (13)$$

with the matrix commutator

$$[\mathbf{A}(q), \mathbf{E}(q)] = \mathbf{A}(q) \mathbf{E}(q) - \mathbf{E}(q) \mathbf{A}(q).$$

We call

$$F_{\text{BO}} = -\langle \boldsymbol{\theta}, \nabla_q \mathbf{E}(q) \boldsymbol{\theta} \rangle \quad (14)$$

the Born–Oppenheimer part of the Hellmann–Feynman force (13).

If all (real) elements of the diagonal matrix $\mathbf{E}(q)$ are different, then the quantum adiabatic theorem [10, 17] implies that the transformed “wave” vector $\boldsymbol{\theta}(t)$ follows the solutions of the reduced system (12) and the motion in the classical degrees of freedom is obtained by time-averaging the Hellmann–Feynman force (13) over the highly oscillatory solutions⁴ $\boldsymbol{\theta}(t)$ of (12). For this, it is crucial to observe that the matrix commutator $[\mathbf{A}(q) \mathbf{E}(q)]$ has zero diagonal entries and, thus, the time average of $\langle \boldsymbol{\theta}(t), [\mathbf{A}(q) \mathbf{E}(q)] \boldsymbol{\theta}(t) \rangle$ is approximately zero. Thus we obtain the averaged system

$$\dot{\boldsymbol{\theta}} = -\frac{i}{\hbar} \mathbf{E}(q) \boldsymbol{\theta},$$

$$\dot{q} = M^{-1} p,$$

$$\dot{p} = -\langle \boldsymbol{\theta}, \nabla_q \mathbf{E}(q) \boldsymbol{\theta} \rangle - \nabla_q U(q).$$

⁴ The average is taken over a period of time T such that (i) $q(t) \approx \text{const.}$ and (ii) the Schrödinger equation (12) undergoes many oscillations. For example, $T \sim \sqrt{\hbar}$ as $\hbar \rightarrow 0$.

Since $\mathbf{E}(q)$ is diagonal, the entries $\theta_i(t) \in \mathcal{C}$, $i = 1, \dots, d$, of the vector $\boldsymbol{\theta}(t)$ satisfy $|\theta_i(t)|^2 = \text{const.}$ and

$$\begin{aligned}\dot{q} &= M^{-1} p, \\ \dot{p} &= - \sum_i |\theta_i|^2 \nabla_q E_{ii}(q) - \nabla_q U(q).\end{aligned}$$

These equations are known as the Born–Oppenheimer approximation for the classical coordinate [16].

If eigenvalues of the matrix $\mathbf{E}(q)$ cross, then $|\theta_i(t)|^2 \neq \text{const.}$, in general, and the Born–Oppenheimer approximation breaks down. In this case, the full QCMD model has to be solved. Note that the crossing of eigenvalues cannot be avoided in general.

EXAMPLE 2. Let us consider a simple toy problem with two fast modes and one slow mode,

$$\begin{aligned}\mathbf{H}(q) &= \begin{bmatrix} q \cos^2 q + (1-q) \sin^2 q & (1-2q) \sin q \cos q \\ (1-2q) \sin q \cos q & q \sin^2 q + (1-q) \cos^2 q \end{bmatrix}, \\ &= \begin{bmatrix} \cos q & \sin q \\ -\sin q & \cos q \end{bmatrix} \begin{bmatrix} q & 0 \\ 0 & 1-q \end{bmatrix} \begin{bmatrix} \cos q & -\sin q \\ \sin q & \cos q \end{bmatrix}\end{aligned}$$

and

$$\mathcal{H} = \frac{1}{2} p^2 + \frac{1}{2} q^2 + \langle \boldsymbol{\psi}, \mathbf{H}(q) \boldsymbol{\psi} \rangle,$$

$q, p \in \mathcal{R}$, $\boldsymbol{\psi} \in \mathcal{C}^2$. Note that

$$\mathbf{Q}(q) = \begin{bmatrix} \cos q & -\sin q \\ \sin q & \cos q \end{bmatrix},$$

$$\mathbf{E}(q) = \begin{bmatrix} q & 0 \\ 0 & 1-q \end{bmatrix},$$

and

$$\mathbf{A} = \begin{bmatrix} 0 & -1 \\ 1 & 0 \end{bmatrix}.$$

Thus the transformed equations of motion are

$$\begin{aligned}\dot{\boldsymbol{\theta}} &= -\frac{i}{\hbar} \mathbf{E}(q) \boldsymbol{\theta} + p \mathbf{A} \boldsymbol{\theta}, \\ \dot{q} &= p, \\ \dot{p} &= -q - \langle \boldsymbol{\theta}, \mathbf{B} \boldsymbol{\theta} \rangle + \langle \boldsymbol{\theta}, \mathbf{C}(q) \boldsymbol{\theta} \rangle,\end{aligned}$$

with

$$\mathbf{B} = \begin{bmatrix} 1 & 0 \\ 0 & -1 \end{bmatrix}$$

and

$$\mathbf{C}(q) = [\mathbf{A}, \mathbf{E}(q)] = \begin{bmatrix} 0 & 2q - 1 \\ 2q - 1 & 0 \end{bmatrix}.$$

The Hellmann–Feynman force (13) is given by

$$F_{\text{HF}} = -\langle \boldsymbol{\theta}, \mathbf{B}\boldsymbol{\theta} \rangle + \langle \boldsymbol{\theta}, \mathbf{C}(q)\boldsymbol{\theta} \rangle. \quad (15)$$

Unless $q \approx 0.5$ (resonance point), the equations can be averaged and we obtain the Born–Oppenheimer system

$$\begin{aligned} \dot{\boldsymbol{\theta}} &= -\frac{i}{\hbar} \mathbf{E}(q)\boldsymbol{\theta}, \\ \dot{q} &= M^{-1}p, \\ \dot{p} &= -q - \langle \boldsymbol{\theta}, \mathbf{B}\boldsymbol{\theta} \rangle. \end{aligned}$$

Numerical results are presented in Section 6.

4. MULTIPLE TIME SCALES IN CLASSICAL MOLECULAR DYNAMICS

4.1. A CMD Model

We now come back to the CMD model of Section 2. In particular, we consider a conservative system with Hamiltonian

$$\mathcal{H}_K = \frac{1}{2} \mathbf{p}^T \mathbf{M}^{-1} \mathbf{p} + \mathcal{V}(\mathbf{q}) + \frac{K}{2} \mathbf{g}(\mathbf{q})^T \mathbf{g}(\mathbf{q}), \quad (16)$$

where $\mathcal{V}: \mathcal{R}^n \rightarrow \mathcal{R}$ and $\mathbf{g}: \mathcal{R}^n \rightarrow \mathcal{R}^m$, $m < n$, are nonnegative functions, $\mathbf{M} \in \mathcal{R}^{n \times n}$ is a diagonal mass matrix, and $K \gg 1$ is a parameter.⁵ We are interested in the limit $K \rightarrow \infty$ and solutions with energy $\mathcal{H}_K \leq c$ for all K sufficiently large; $c > 0$ some given constant. This implies that each component $g_i(\mathbf{q})$, $i = 1, \dots, m$, of the vector-valued function \mathbf{g} satisfies

$$g_i(\mathbf{q}) \leq \sqrt{\frac{2c}{K}}$$

and, for $K \rightarrow \infty$, suggests replacing the equations of motion

$$\begin{aligned} \dot{\mathbf{q}} &= \mathbf{M}^{-1} \mathbf{p}, \\ \dot{\mathbf{p}} &= -\nabla_{\mathbf{q}} \mathcal{V}(\mathbf{q}) - K \mathbf{G}(\mathbf{q})^T \mathbf{g}(\mathbf{q}), \end{aligned}$$

$\mathbf{G}(\mathbf{q}) \in \mathcal{R}^{m \times n}$ the Jacobian of $\mathbf{g}(\mathbf{q})$, with the constrained system

$$\dot{\mathbf{q}} = \mathbf{M}^{-1} \mathbf{p}, \quad (17)$$

$$\dot{\mathbf{p}} = -\nabla_{\mathbf{q}} \mathcal{V}(\mathbf{q}) - \mathbf{G}(\mathbf{q})^T \boldsymbol{\lambda}, \quad (18)$$

$$\mathbf{0} = \mathbf{g}(\mathbf{q}). \quad (19)$$

We assume throughout the paper that the $m \times m$ matrix $\mathbf{G}(\mathbf{q})\mathbf{M}^{-1}\mathbf{G}(\mathbf{q})^T$ is invertible.

⁵ This Hamiltonian corresponds to the general system considered in Section 2 except that all force constants $\{k_{ii}\}$ are assumed to be equal to K and the number of degrees of freedom satisfies $n = 3N$.

The constrained system can be integrated numerically using the SHAKE and RATTLE methods [2, 37], which are basically equivalent [27] and lead to a modified Verlet method of type

$$\begin{aligned}\mathbf{q}_{n+1} &= \mathbf{q}_n + \Delta t \mathbf{M}^{-1} \mathbf{p}_{n+1/2}, \\ \mathbf{p}_{n+1/2} &= \mathbf{p}_n - \frac{\Delta t}{2} \nabla_{\mathbf{q}} \mathcal{V}(\mathbf{q}_n) - \Delta t \mathbf{G}(\mathbf{q}_n)^T \boldsymbol{\lambda}_n, \\ \mathbf{p}_{n+1} &= \mathbf{p}_{n+1/2} - \frac{\Delta t}{2} \nabla_{\mathbf{q}} \mathcal{V}(\mathbf{q}_{n+1}), \\ \mathbf{0} &= \mathbf{g}(\mathbf{q}_{n+1}).\end{aligned}$$

Although this approach is very appealing, the constrained system does not, in general, reflect the correct limit behavior of the unconstrained system for $K \gg 1$. There are basically two problems:

- Even in the limit $K \rightarrow \infty$, solutions of (16) do not, in general, reduce to solutions of the constrained system (17)–(19). This is due to a coupling of the fast oscillations to the slowly varying solution components. This coupling gives rise to an additional (correcting) force term in (17)–(19). See [11, 14, 32, 36, 41] and Section 4.3 below.
- The approximation $g_i(\mathbf{q}) = 0$ is often too crude unless the force constant K is very large. In fact, the function values g_i rapidly oscillate about the minimum of the total energy (16). This leads to a modified constrained function in (19). The numerical implementation of these “soft constraints” has been discussed in [33, 44]. An equivalent (but somewhat easier to implement) approach is to modify the force field [35].

A brief account of the relevant analysis leading to the correcting potential is given in the following section. The approach is new in the sense that we show the relation of the unconstrained formulation to the QCMD model. This allows us to restrict the analysis of the limiting behavior to the limiting behavior of a QCMD-like model (as discussed in Section 3).

4.2. Reduction of the CMD Model to a QCMD-like Model

The underlying QCMD model is found by a sequence of canonical transformations [3] of phase space. We start with the canonical point transformation introduced by the coordinate transformation

$$\begin{aligned}\mathbf{q}_1 &:= \mathbf{g}(\mathbf{q}), \\ \mathbf{q}_2 &:= \mathbf{b}(\mathbf{q}),\end{aligned}$$

where $\mathbf{b}: \mathcal{R}^n \rightarrow \mathcal{R}^{n-m}$ is an appropriate function such that $\mathbf{B}(\mathbf{q})\mathbf{M}^{-1}\mathbf{G}(\mathbf{q})^T = \mathbf{0}$. Here $\mathbf{B}(\mathbf{q}) \in \mathcal{R}^{(n-m) \times n}$ denotes the Jacobian of the function $\mathbf{b}(\mathbf{q})$. The corresponding conjugate momenta are defined via the relation

$$\mathbf{p} = \mathbf{G}(\mathbf{q})^T \mathbf{p}_1 + \mathbf{B}(\mathbf{q})^T \mathbf{p}_2.$$

Using this transformation, the Hamiltonian (16) becomes

$$\begin{aligned}\mathcal{H}_K &= \frac{1}{2} \mathbf{p}_1^T \mathbf{G}(\mathbf{q}) \mathbf{M}^{-1} \mathbf{G}(\mathbf{q})^T \mathbf{p}_1 + \frac{1}{2} \mathbf{p}_2^T \mathbf{B}(\mathbf{q}) \mathbf{M}^{-1} \mathbf{B}(\mathbf{q})^T \mathbf{p}_2 + \mathcal{V}(\mathbf{q}) + \frac{K}{2} \mathbf{q}_1^T \mathbf{q}_1, \\ &= \frac{1}{2} \mathbf{p}_1^T \mathbf{A}(\mathbf{q}_1, \mathbf{q}_2) \mathbf{p}_1 + \frac{1}{2} \mathbf{p}_2^T \mathbf{C}(\mathbf{q}_1, \mathbf{q}_2) \mathbf{p}_2 + \mathcal{W}(\mathbf{q}_1, \mathbf{q}_2) + \frac{K}{2} \mathbf{q}_1^T \mathbf{q}_1\end{aligned}$$

with $\mathbf{A}(\mathbf{q}_1, \mathbf{q}_2) = \mathbf{G}(\mathbf{q})\mathbf{M}^{-1}\mathbf{G}(\mathbf{q})^T$, $\mathbf{C}(\mathbf{q}_1, \mathbf{q}_2) = \mathbf{B}(\mathbf{q})\mathbf{M}^{-1}\mathbf{B}(\mathbf{q})^T$, and $\mathcal{W}(\mathbf{q}_1, \mathbf{q}_2) = \mathcal{V}(\mathbf{q})$. Since the components $\{q_{1,i}\}_{i=1,\dots,m}$ of the vector \mathbf{q}_1 satisfy

$$q_{1,i} \leq \sqrt{\frac{2c}{K}},$$

we can scale \mathbf{q}_1 by $K^{1/2}$ and define $\tilde{\mathbf{q}}_1 := K^{1/2}\mathbf{q}_1$. This yields the Hamiltonian

$$\mathcal{H}_\epsilon = \frac{1}{2}\mathbf{p}_1^T \mathbf{A}(\epsilon\tilde{\mathbf{q}}_1, \mathbf{q}_2)\mathbf{p}_1 + \frac{1}{2}\mathbf{p}_2^T \mathbf{C}(\epsilon\tilde{\mathbf{q}}_1, \mathbf{q}_2)\mathbf{p}_2 + \mathcal{W}(\epsilon\tilde{\mathbf{q}}_1, \mathbf{q}_2) + \frac{1}{2}\tilde{\mathbf{q}}_1^T \tilde{\mathbf{q}}_1 \quad \text{with } \epsilon := K^{-1/2}. \quad (20)$$

The equations of motion are generated via the scaled Lie–Poisson bracket

$$\{F, G\} = \epsilon^{-1}\{F, G\}_{\tilde{\mathbf{q}}_1, \mathbf{p}_1} + \{F, G\}_{\mathbf{q}_2, \mathbf{p}_2}.$$

Here $\{F, G\}_{\tilde{\mathbf{q}}_1, \mathbf{p}_1}$ and $\{F, G\}_{\mathbf{q}_2, \mathbf{p}_2}$ denote again the canonical bracket of classical mechanics. Note that the constrained dynamics is obtained by setting $\tilde{\mathbf{q}}_1 = \mathbf{0}$ and $\mathbf{p}_1 = \mathbf{0}$. Thus, in local coordinates, the constrained system (17)–(19) is characterized by the Hamiltonian

$$\mathcal{H}_c = \frac{1}{2}\mathbf{p}_2^T \mathbf{K}(\mathbf{q}_2)\mathbf{p}_2 + W(\mathbf{q}_2) \quad (21)$$

with $\mathbf{K}(\mathbf{q}_2) = \mathbf{C}(\mathbf{0}, \mathbf{q}_2)$ and $W(\mathbf{q}_2) = \mathcal{W}(\mathbf{0}, \mathbf{q}_2)$.

Without giving a rigorous justification, we now set the (small) term $\epsilon\tilde{\mathbf{q}}_1$ in the Hamiltonian (20) equal to zero. This yields

$$\mathcal{H}_0 = \frac{1}{2}\mathbf{p}_1^T \mathbf{A}(\mathbf{0}, \mathbf{q}_2)\mathbf{p}_1 + \frac{1}{2}\mathbf{p}_2^T \mathbf{K}(\mathbf{q}_2)\mathbf{p}_2 + W(\mathbf{q}_2) + \frac{1}{2}\tilde{\mathbf{q}}_1^T \tilde{\mathbf{q}}_1, \quad (22)$$

which is to be compared to the constrained Hamiltonian (21). Next we introduce the matrix-valued function $\mathbf{D}(\mathbf{q}_2) \in \mathcal{R}^{m \times m}$ by

$$\mathbf{D}(\mathbf{q}_2) = [\mathbf{A}(\mathbf{0}, \mathbf{q}_2)]^{1/4}.$$

This gives rise to another canonical point transformation via the coordinate transformation

$$\begin{aligned} \mathbf{x} &= \mathbf{D}(\mathbf{q}_2)^{-1}\tilde{\mathbf{q}}_1, \\ \mathbf{y} &= \mathbf{q}_2 \end{aligned}$$

and corresponding canonical momenta $(\mathbf{p}_x, \mathbf{p}_y)$ defined by

$$\begin{bmatrix} \mathbf{D}(\mathbf{q}_2)^{-1} & \mathbf{0} \\ -\epsilon \left[\frac{\partial}{\partial \mathbf{q}_2} \mathbf{D}(\mathbf{q}_2)^{-1} \tilde{\mathbf{q}}_1 \right]^T & \mathbf{I} \end{bmatrix} \begin{bmatrix} \mathbf{p}_x \\ \mathbf{p}_y \end{bmatrix} = \begin{bmatrix} \mathbf{p}_1 \\ \mathbf{p}_2 \end{bmatrix}. \quad (23)$$

Upon dropping the off-diagonal term of order ϵ in (23), the Hamiltonian (22) becomes

$$\mathcal{H}_0 = \frac{1}{2}\mathbf{p}_x^T \mathbf{H}(\mathbf{y})\mathbf{p}_x + \frac{1}{2}\mathbf{p}_y^T \mathbf{K}(\mathbf{y})\mathbf{p}_y + W(\mathbf{y}) + \frac{1}{2}\mathbf{x}^T \mathbf{H}(\mathbf{y})\mathbf{x},$$

with $\mathbf{H}(\mathbf{y}) = \mathbf{D}(\mathbf{y})^2$ and $\mathbf{K}(\mathbf{y})$, $W(\mathbf{y})$ as defined in (21). The corresponding Lie–Poisson bracket is

$$\{F, G\} = \epsilon^{-1}\{F, G\}_{\mathbf{x}, \mathbf{p}_\mathbf{x}} + \{F, G\}_{\mathbf{y}, \mathbf{p}_\mathbf{y}}.$$

Next we consider \mathbf{x} and $\mathbf{p}_\mathbf{x}$ as the real and imaginary part of the complex vector $\mathbf{z} \in \mathcal{C}^m$, i.e.,

$$\mathbf{z} = \frac{1}{\sqrt{2}}(\mathbf{x} + i\mathbf{p}_\mathbf{x}).$$

This yields

$$\mathcal{H}_0 = \bar{\mathbf{z}}^T \mathbf{H}(\mathbf{y})\mathbf{z} + \frac{1}{2}\mathbf{p}_\mathbf{y}^T \mathbf{K}(\mathbf{y})\mathbf{p}_\mathbf{y} + W(\mathbf{y}),$$

and we write this as a QCMD-like system with total energy

$$\mathcal{H}_0 = \langle \mathbf{z}, \mathbf{H}(\mathbf{y})\mathbf{z} \rangle + \mathcal{H}_c(\mathbf{y}, \mathbf{p}_\mathbf{y}),$$

the finite-dimensional ‘‘Schrödinger operator’’ $\mathbf{H}(\mathbf{y})$, the ‘‘wave function’’ \mathbf{z} , the artificial ‘‘Planck constant’’ ϵ , and the classical (constrained) Hamiltonian (21). The equations of motion are

$$\dot{\mathbf{z}} = -\frac{i}{\epsilon}\mathbf{H}(\mathbf{y})\mathbf{z}, \tag{24}$$

$$\dot{\mathbf{y}} = +\nabla_{\mathbf{p}_\mathbf{y}}\mathcal{H}_c(\mathbf{y}, \mathbf{p}_\mathbf{y}), \tag{25}$$

$$\dot{\mathbf{p}}_\mathbf{y} = -\nabla_{\mathbf{y}}\mathcal{H}_c(\mathbf{y}, \mathbf{p}_\mathbf{y}) - \nabla_{\mathbf{y}}\langle \mathbf{z}, \mathbf{H}(\mathbf{y})\mathbf{z} \rangle. \tag{26}$$

We are interested in the limit $\epsilon \rightarrow 0$, which we will discuss in Section 4.3. The constrained system approximation corresponds to $\mathcal{H}_0 = \mathcal{H}_c$, which neglects the ‘‘quantum’’ contributions. We note that $I := \langle \mathbf{z}, \mathbf{z} \rangle$ is a first integral of the system. The same quantity is not necessarily conserved for the system with the complete Hamiltonian (20).⁶ However, numerical experiments indicate that I is an adiabatic invariant for \mathcal{H}_ϵ and is conserved over relatively long integration intervals up to small fluctuations. See Example 3 below. A theoretical investigation of this behavior will be carried out in a forthcoming publication.

EXAMPLE 3. We consider a planar system consisting of six particles with coordinates $\mathbf{q}_i \in \mathcal{R}^2$ and mass $m = 1$. The particles interact with one another through a (stiff) harmonic potential

$$\mathcal{V}_{\text{stiff}} = \frac{K}{2} \sum_{j=0}^5 (r_{j,j+1} - 1)^2,$$

$r_{ij} = \|\mathbf{q}_i - \mathbf{q}_j\|$, and a (soft) anharmonic potential

$$\mathcal{V}_{\text{soft}} = \sum_{j=0}^4 \sum_{i=j+2}^6 \frac{1}{r_{ij}}.$$

⁶ We have $\mathcal{H}_\epsilon = \mathcal{H}_0 + \mathcal{O}(\epsilon)$.

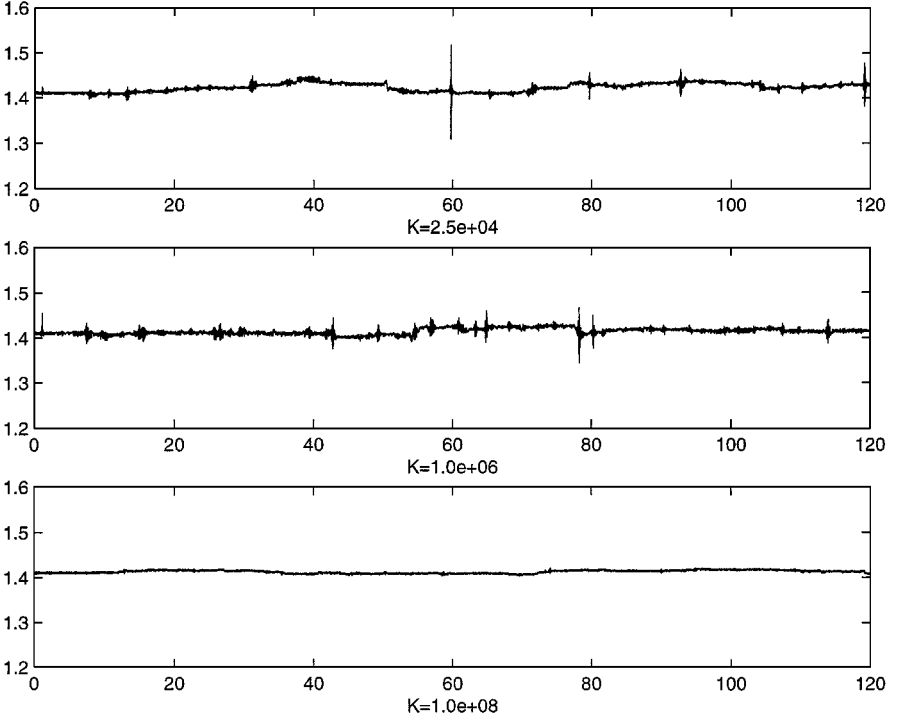


FIG. 1. Time evolution of $I(t)$ over a time interval $[0, 120]$ for different values of the force constant K .

For simplicity, the first particle is fixed at zero. The force constant K is set to $K = 2.5 \times 10^4$, 1.0×10^6 , and 1.0×10^8 . We integrate the equations of motion using the Verlet method with a sufficiently small step size of $\Delta t = 0.1/\sqrt{K}$ and compute the eigenvalues of the corresponding matrix $\mathbf{H}(\mathbf{y}) \in \mathcal{R}^{5 \times 5}$, the entries of the vector $\mathbf{z} \in \mathcal{C}^5$, and $I = \langle \mathbf{z}, \mathbf{z} \rangle$. In Fig. 1, we plot the time evolution of $I(t)$ over a time interval $T = 120$. It can be concluded that the norm of the vector \mathbf{z} is relatively well conserved for our two-time-scales CMD model. Numerical results on the time evolution of the individual entries of the vector \mathbf{z} can be found in Section 4.3.

In terms of the original variables (\mathbf{q}, \mathbf{p}) , the QCMD-like equations (24)–(26) can be written as a constrained QCMD-like system

$$\begin{aligned} \dot{\mathbf{z}} &= -\frac{i}{\epsilon} \mathbf{H}(\mathbf{q}) \mathbf{z}, \\ \dot{\mathbf{q}} &= \mathbf{M}^{-1} \mathbf{p}, \\ \dot{\mathbf{p}} &= -\nabla_{\mathbf{q}} \mathcal{V}(\mathbf{q}) - \nabla_{\mathbf{q}} \langle \mathbf{z}, \mathbf{H}(\mathbf{q}) \mathbf{z} \rangle - \mathbf{G}(\mathbf{q})^T \lambda, \\ \mathbf{0} &= \mathbf{g}(\mathbf{q}), \end{aligned}$$

with $\mathbf{H}(\mathbf{q}) = [\mathbf{G}(\mathbf{q}) \mathbf{M}^{-1} \mathbf{G}(\mathbf{q})^T]^{1/2}$.

4.3. The Limiting Behavior of the CMD Model

The results of the previous section indicate that one can reduce the discussion of the limiting behavior of the CMD model as $\epsilon = K^{-1/2} \rightarrow 0$ to the investigation of the QCMD-like equations (24)–(26).

In case that $\mathbf{H}(\mathbf{y})$ is a scalar, i.e., $\mathbf{H}(\mathbf{y}) = h(\mathbf{y}) \in \mathcal{R}$, no resonances can occur and the “Born–Oppenheimer” approximation is valid for all \mathbf{y} . The averaged equations are

$$\begin{aligned}\dot{\mathbf{y}} &= +\nabla_{\mathbf{p}_y} \mathcal{H}_c(\mathbf{y}, \mathbf{p}_y), \\ \dot{\mathbf{p}}_y &= -\nabla_{\mathbf{y}} \mathcal{H}_c(\mathbf{y}, \mathbf{p}_y) - |z|^2 \nabla_{\mathbf{y}} h(\mathbf{y}), \\ |z|^2 &= \text{const.}\end{aligned}$$

The need for the correcting force term $F_c = |z|^2 \nabla_{\mathbf{y}} h(\mathbf{y})$ was first pointed out by Rubin and Ungar [36]. It was shown in [34] that the corresponding CMD equations satisfy $|z(t)| \approx \text{const.}$ over an exponentially long-time interval $T \sim e^{c/\epsilon}$, $c > 0$ some constant, if the energy function (16) is real analytic.

Under the assumption that the fast degree of motion is strongly coupled to a heat bath with temperature T , the correcting force term is determined by the relation $|z|^2 h(\mathbf{y}) = k_B T$ and leads to the Fixman potential $V_c = k_B T \ln h(\mathbf{y})$ [18, 32].

If a given matrix-valued $\mathbf{H}(\mathbf{y})$ can be smoothly diagonalized, then we can still apply the “Born–Oppenheimer” approximation provided the eigenvalues of the matrix $\mathbf{H}(\mathbf{y})$ are all different. This case was first investigated by Takens in [41]. For a recent discussion in terms of homogenization see [11]. If eigenvalues cross, then the “Born–Oppenheimer” approximation breaks down as for the QCMD model of Section 3. See the numerical example below.

The correcting force term vanishes if $\mathbf{H}(\mathbf{y}) = \mathbf{H} = \text{const.}$ This situation occurs if the constrained Hamiltonian (21) corresponds to a system of uncoupled rigid bodies, i.e., $\mathbf{G}(\mathbf{q})\mathbf{M}^{-1}\mathbf{G}(\mathbf{q})^T = \text{const.}$, and has been analyzed by Benettin *et al.* in [5].

EXAMPLE 3 (Continued). In Fig. 2, we present the eigenvalues of the “Schrödinger” matrix $\mathbf{H}(\mathbf{y})$ and the “occupation numbers” $|z_i(t)|^2$, $i = 1, \dots, 5$, corresponding to the “wave” vector $\mathbf{z}(t)$. The force constant was set equal to $K = 2.5 \times 10^4$. “Occupation numbers” $|z_i(t)|^2$ jump when the corresponding eigenvalues undergo or are close to a 1:1 resonance (except at $t \approx 22.2$). It should be noted that higher-order resonances do not lead to transitions in the “occupation numbers.” This is contrary to what can be expected from the results presented in [11, 41].

5. MULTIPLE TIME STEPPING FOR CLASSICAL MOLECULAR DYNAMICS

The analysis of Section 4 indicates that in most cases the fast oscillations cannot be eliminated (or ignored) in long-term MD simulations. In particular, non-adiabatic transitions and the breakdown of the “Born–Oppenheimer” approximation are unavoidable. The best way out might be an efficient simulation of the full system which takes into account the existing multiple time scales. Since the standard MTS method (5) suffers from resonance induced instabilities [7], we will discuss a variant of the mollified MTS methods, as suggested in [19], that is particularly suited for the CMD model.

5.1. Projected Multiple Time Stepping

Let us come back to highly oscillatory Hamiltonian systems of type

$$\begin{aligned}\dot{\mathbf{q}} &= \mathbf{M}^{-1}\mathbf{p}, \\ \dot{\mathbf{p}} &= -\nabla_{\mathbf{q}} \mathcal{V}(\mathbf{q}) - \mathbf{G}(\mathbf{q})^T \mathbf{K}\mathbf{g}(\mathbf{q}).\end{aligned}$$

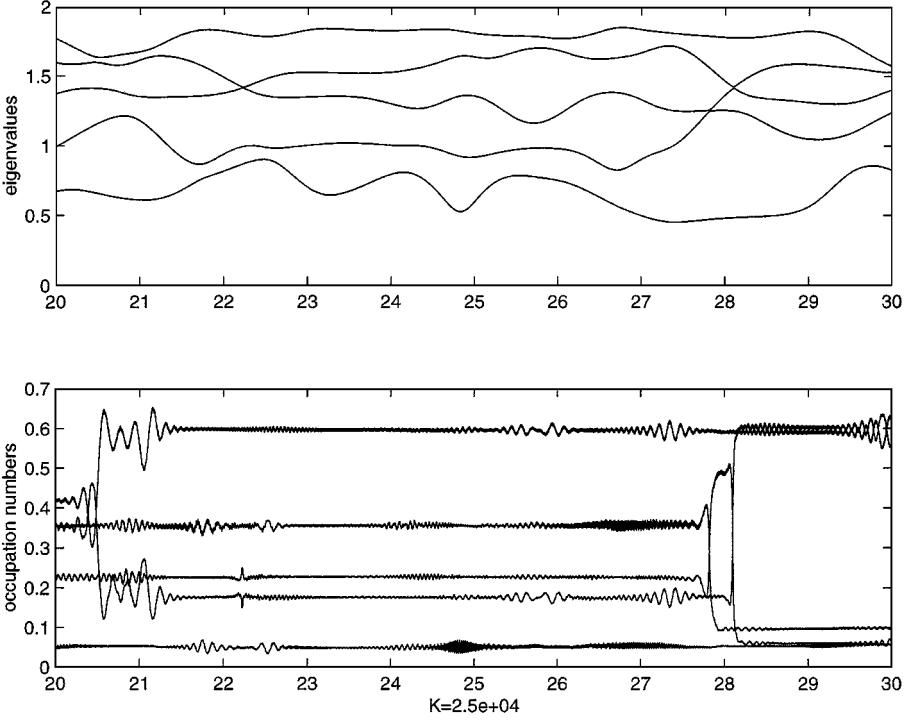


FIG. 2. Time evolution of the eigenvalues of $\mathbf{H}(\mathbf{y})$ and the corresponding “occupation numbers” $|z_i(t)|^2$, $i = 1, \dots, 5$, for $K = 2.5 \times 10^4$ and over the time interval $[20, 30]$.

The Hamiltonian is

$$\mathcal{H}(\mathbf{q}, \mathbf{p}) = \frac{\mathbf{p}^T \mathbf{M}^{-1} \mathbf{p}}{2} + \mathcal{V}(\mathbf{q}) + \frac{\mathbf{g}(\mathbf{q})^T \mathbf{K} \mathbf{g}(\mathbf{q})}{2}$$

and we split the potential energy \mathcal{V} into a short range contribution \mathcal{V}_1 and a long-range contribution \mathcal{V}_2 . The standard MTS method [7, 23, 42] is now defined via the splitting

$$\mathcal{H} = T(\mathbf{p}) + U_1(\mathbf{q}) + U_2(\mathbf{q}),$$

with $U_2 = \mathcal{V}_2$ and $U_1 = \mathcal{V}_1 + 1/2 \mathbf{g}(\mathbf{q})^T \mathbf{K} \mathbf{g}(\mathbf{q})$. This leads to the MTS algorithm (5), which is more explicitly written out in Fig. 3.

This formulation suffers from resonance-induced instabilities [7, 9], which are caused by an unfortunate sampling of the high-frequency oscillations in $\mathbf{q}_1 = \mathbf{g}(\mathbf{q})$. In [19], García-Archilla *et al.* suggested combining averaging with multiple time stepping. Here we use information about the analytical solution behavior of the fast system to obtain the averaged force field.

The motion in $\mathbf{q}_1 := \mathbf{g}(\mathbf{q})$ is highly oscillatory with a time average close to zero. To eliminate the effect of the highly oscillatory variable \mathbf{q}_1 on the long-range forces in (5), we replace the long-range force field $\mathbf{F}_2(\mathbf{q}) = -\nabla_{\mathbf{q}} U_2(\mathbf{q})$ by

$$\bar{\mathbf{F}}_2(\mathbf{q}) = -\nabla_{\mathbf{q}} U_2(\psi(\mathbf{q})),$$

which is the gradient of the modified potential energy $\mathbf{W}(\mathbf{q}) := U_2(\psi(\mathbf{q}))$.

Step 1.

$$\bar{\mathbf{p}}_n = \mathbf{p}_n - \frac{\Delta t}{2} \nabla_{\mathbf{q}} U_2(\mathbf{q}_n)$$

Step 2.

Integrate the fast/local system

$$\begin{aligned} \frac{d}{dt} \mathbf{q} &= \mathbf{M}^{-1} \mathbf{p}, \\ \frac{d}{dt} \mathbf{p} &= -\nabla_{\mathbf{q}} U_1(\mathbf{q}) \end{aligned}$$

using Verlet with a step-size $\delta t = \Delta t/j$, $j \gg 1$, and initial conditions $(\mathbf{q}_n, \bar{\mathbf{p}}_n)$. Denote the result by $(\mathbf{q}_{n+1}, \bar{\mathbf{p}}_{n+1})$.

Step 3.

$$\mathbf{p}_{n+1} = \bar{\mathbf{p}}_{n+1} - \frac{\Delta t}{2} \nabla_{\mathbf{q}} U_2(\mathbf{q}_{n+1})$$

FIG. 3. Standard multiple time stepping.

The function ψ is defined by the SHAKE-like nonlinear system of equations

$$\begin{aligned} \tilde{\mathbf{q}} &= \psi(\mathbf{q}) = \mathbf{q} + \mathbf{M}^{-1} \mathbf{G}(\mathbf{q})^T \boldsymbol{\mu}, \\ \mathbf{0} &= \mathbf{g}(\tilde{\mathbf{q}}) \end{aligned}$$

in the variable $\boldsymbol{\mu} \in \mathcal{R}^m$. Note that ψ projects the $\mathbf{q}_1 = \mathbf{g}(\mathbf{q})$ solution component to zero. To implement our approach, we need the Jacobian $\partial_{\mathbf{q}} \psi$ of ψ . This requires the computation of the second derivative $\partial_{\mathbf{q}\mathbf{q}} g_i(\mathbf{q})$ of the functions g_i , $i = 1, \dots, m$, and the solution of a linear system of equations, i.e.,

$$\begin{aligned} \mathbf{d}\tilde{\mathbf{q}} &= \mathbf{d}\mathbf{q} + \mathbf{M}^{-1} \mathbf{G}(\mathbf{q})^T \mathbf{d}\boldsymbol{\mu} + \mathbf{M}^{-1} \sum_{i=1}^m \mu_i \partial_{\mathbf{q}\mathbf{q}} g_i(\mathbf{q}) \mathbf{d}\mathbf{q}, \\ \mathbf{0} &= \mathbf{G}(\tilde{\mathbf{q}}) \mathbf{d}\tilde{\mathbf{q}} \end{aligned}$$

with $\tilde{\mathbf{q}} = \psi(\mathbf{q})$ and $\mathbf{d}\tilde{\mathbf{q}} = \partial_{\mathbf{q}} \psi(\mathbf{q}) \mathbf{d}\mathbf{q}$, or, in other words,

$$\partial_{\mathbf{q}} \psi(\mathbf{q}) = [\mathbf{I} - \mathbf{M}^{-1} \mathbf{G}(\mathbf{q})^T \Omega \mathbf{G}(\tilde{\mathbf{q}})] \left[\mathbf{I} + \mathbf{M}^{-1} \sum_{i=1}^m \mu_i \partial_{\mathbf{q}\mathbf{q}} g_i(\mathbf{q}) \right]$$

with

$$\Omega := [\mathbf{G}(\tilde{\mathbf{q}}) \mathbf{M}^{-1} \mathbf{G}(\mathbf{q})^T]^{-1}.$$

This leads us to the projected MTS scheme of Fig. 4 [26, 34].

This symplectic scheme avoids the resonance problems typically encountered in the standard MTS method and is useful whenever the evaluation of $\nabla_{\mathbf{q}} U_2(\mathbf{q})$ (long-range forces) is much more expensive than the evaluation of $\nabla_{\mathbf{q}} U_1(\mathbf{q})$.

The modified MTS method of García-Archilla *et al.*, as well as our projected multiple-time-stepping method, has been tested for a box of water. Both methods allow one to increase

Step 1.

$$\begin{aligned}\tilde{\mathbf{q}}_n &= \psi(\mathbf{q}_n), \\ \mathbf{F}_n &= -[\partial_{\mathbf{q}}\psi(\mathbf{q}_n)]^T \nabla_{\tilde{\mathbf{q}}}U_2(\tilde{\mathbf{q}}_n)\end{aligned}$$

Step 2.

$$\bar{\mathbf{p}}_n = \mathbf{p}_n + \frac{\Delta t}{2}\mathbf{F}_n$$

Step 3.

Integrate the fast system

$$\begin{aligned}\frac{d}{dt}\mathbf{q} &= \mathbf{M}^{-1}\mathbf{p}, \\ \frac{d}{dt}\mathbf{p} &= -\nabla_{\mathbf{q}}U_1(\mathbf{q})\end{aligned}$$

using Verlet with a step-size $\delta t = \Delta t/j$, $j \gg 1$, and initial conditions $(\mathbf{q}_n, \bar{\mathbf{p}}_n)$. Denote the result by $(\mathbf{q}_{n+1}, \bar{\mathbf{p}}_{n+1})$.

Step 4.

$$\begin{aligned}\tilde{\mathbf{q}}_{n+1} &= \psi(\mathbf{q}_{n+1}), \\ \mathbf{F}_{n+1} &= -[\partial_{\mathbf{q}}\psi(\mathbf{q}_{n+1})]^T \nabla_{\tilde{\mathbf{q}}}U_2(\tilde{\mathbf{q}}_{n+1})\end{aligned}$$

Step 5.

$$\mathbf{p}_{n+1} = \bar{\mathbf{p}}_{n+1} + \frac{\Delta t}{2}\mathbf{F}_{n+1}$$

FIG. 4. Projected multiple-time-stepping method.

the step size Δt from 1–2 to 5–7 fs (1 fs = 10^{-15} s) without any additional evaluation of the long-range forces [26]. In fact, the projection method turns out to be more robust than the methods using averaging [26]. Note that the standard MTS method (5) becomes unstable at $\Delta t \approx 4$ fs. It can be expected that improved projected/averaged MTS methods will allow one to increase the macro step size up to $\Delta t \approx 10$ fs [26].

5.2. A Modified Projection Step

The approximation $\mathbf{g}(\mathbf{q}) = \mathbf{0}$ in the definition of the map ψ might not be suitable for moderate values of the force constants, and a better approximation to the averaged values of $\mathbf{q}_1 = \mathbf{g}(\mathbf{q})$ should be used. As pointed out in [33, 44], the variable \mathbf{q}_1 oscillates about the minimum of the total energy in the direction of \mathbf{q}_1 . This minimum is characterized⁷ by the nonlinear equation

$$\mathbf{0} = \mathbf{G}(\tilde{\mathbf{q}})\mathbf{M}^{-1}\nabla_{\tilde{\mathbf{q}}}U_1(\tilde{\mathbf{q}}),$$

which replaces the constraint $\mathbf{g}(\mathbf{q}) = \mathbf{0}$. Thus we introduce the modified projection

$$\tilde{\mathbf{q}} := \phi(\mathbf{q})$$

⁷ Here we have neglected velocity-dependent contributions and contributions from the long-range potential energy $U_2(\mathbf{q})$.

by means of

$$\begin{aligned}\tilde{\mathbf{q}} &:= \mathbf{q} + \mathbf{M}^{-1}\mathbf{G}(\mathbf{q})^T\boldsymbol{\eta}, \\ \mathbf{0} &= \mathbf{G}(\tilde{\mathbf{q}})\mathbf{M}^{-1}\nabla_{\tilde{\mathbf{q}}}U_1(\tilde{\mathbf{q}}).\end{aligned}\tag{27}$$

The resulting nonlinear system in the variable $\boldsymbol{\eta} \in R^m$ can be solved by Newton's method with the simplified (symmetric) Jacobian

$$\mathbf{J} = [\mathbf{G}(\mathbf{q})\mathbf{M}^{-1}\mathbf{G}(\mathbf{q})^T]\mathbf{K}[\mathbf{G}(\mathbf{q})\mathbf{M}^{-1}\mathbf{G}(\mathbf{q})].$$

As before, we introduce a modified (averaged) long-range potential energy function

$$W(\mathbf{q}) := U_2(\phi(\mathbf{q})).$$

The evaluation of the gradient

$$\nabla_{\mathbf{q}}W(\mathbf{q}) = [\partial_{\mathbf{q}}\phi(\mathbf{q})]^T\nabla_{\tilde{\mathbf{q}}}U_2(\tilde{\mathbf{q}})$$

requires the computation of $\partial_{\mathbf{q}}\phi(\mathbf{q})$, i.e.,

$$\begin{aligned}\mathbf{d}\tilde{\mathbf{q}} &:= \partial_{\mathbf{q}}\phi(\mathbf{q})\mathbf{d}\mathbf{q}, \\ &= \mathbf{d}\mathbf{q} + \mathbf{M}^{-1}\mathbf{G}(\mathbf{q})^T\mathbf{d}\boldsymbol{\eta} + \mathbf{M}^{-1}\sum_{i=1}^m\eta_i\partial_{\mathbf{q}\mathbf{q}}g_i(\mathbf{q})\mathbf{d}\mathbf{q},\end{aligned}$$

and $\mathbf{d}\boldsymbol{\eta}$ is determined by the equation

$$\mathbf{0} = \partial_{\tilde{\mathbf{q}}}\left[\mathbf{G}(\tilde{\mathbf{q}})\mathbf{M}^{-1}\nabla_{\tilde{\mathbf{q}}}U_1(\tilde{\mathbf{q}})\right]\mathbf{d}\tilde{\mathbf{q}}.$$

In terms of the individual functions g_i , this results in

$$0 = \left\{[\mathbf{M}^{-1}\nabla_{\tilde{\mathbf{q}}}U_1(\tilde{\mathbf{q}})]^T\partial_{\tilde{\mathbf{q}}\tilde{\mathbf{q}}}g_i(\tilde{\mathbf{q}}) + \mathbf{G}_i(\tilde{\mathbf{q}})\mathbf{M}^{-1}\partial_{\tilde{\mathbf{q}}\tilde{\mathbf{q}}}U_1(\tilde{\mathbf{q}})\right\}\mathbf{d}\tilde{\mathbf{q}},$$

which includes the computation of the Hessian of $U_1(\mathbf{q})$. Thus this approach should only be used if U_1 is restricted to nearest neighborhood interactions such as the bond stretching/bending potentials and the repulsive part of the Lennard–Jones interactions.

The modified projection can be built into the MTS scheme of Fig. 4 by replacing ψ with ϕ . We point out that this modified force field requires additional force field evaluations. However, these additional force field evaluations are restricted to nearest neighborhood interactions.

6. MULTIPLE TIME STEPPING FOR QUANTUM–CLASSICAL MOLECULAR DYNAMICS

A natural extension [30] of the Verlet method to the QCMD equations of motion is given by

$$\psi_{n+1/2} = \exp\left(-i\frac{\Delta t}{2\hbar}\mathbf{H}(\mathbf{q}_n)\right)\psi_n,\tag{28}$$

$$\text{Leapfrog} \begin{cases} \mathbf{q}_{n+1/2} = \mathbf{q}_n + \frac{\Delta t}{2} \mathbf{M}^{-1} \mathbf{p}_n, \\ \mathbf{p}_{n+1} = \mathbf{p}_n - \Delta t \langle \psi_{n+1/2}, \nabla_{\mathbf{q}} \mathbf{H}(\mathbf{q}_{n+1/2}) \psi_{n+1/2} \rangle - \Delta t \nabla_{\mathbf{q}} U(\mathbf{q}_{n+1/2}), \\ \mathbf{q}_{n+1} = \mathbf{q}_{n+1/2} + \frac{\Delta t}{2} \mathbf{M}^{-1} \mathbf{p}_{n+1}, \end{cases} \quad (29)$$

$$\psi_{n+1} = \exp\left(-i \frac{\Delta t}{2\hbar} \mathbf{H}(\mathbf{q}_{n+1})\right) \psi_{n+1/2}. \quad (30)$$

Even if the matrix exponentials in (28) and (30) are evaluated exactly, the scheme requires a very small step size. Otherwise the Hellmann–Feynman forces acting on the classical coordinates will be wrongly approximated [24, 30, 31] and the behavior of the populations $\{|\theta_i(t)|^2\}$ may not be reproduced correctly (see Example 4 below). The same holds true for MTS variants of the above method, as suggested in [38, 39], where the matrix exponential is replaced by an approximation using j steps of a smaller step size $\delta t = \Delta t/j$.

EXAMPLE 4. We demonstrate a potentially dangerous implication of using a large time step on the preservation of the populations $\{|\theta_i(t)|^2\}$ in an adiabatic regime. Let us consider a simple two-dimensional system

$$\dot{\psi} = -\frac{i}{\hbar} \mathbf{H}(t) \psi, \quad (31)$$

$\psi \in \mathcal{C}^2$, where the dependence of \mathbf{H} on the classical coordinate q is replaced by a time dependence. In particular, we take

$$\mathbf{H}(t) = \begin{bmatrix} \cos^2 t - \sin^2 t & -2 \cos t \sin t \\ -2 \cos t \sin t & \sin^2 t - \cos^2 t \end{bmatrix}$$

and introduce a new vector θ ,

$$\theta = \mathbf{Q}(t) \psi,$$

with

$$\mathbf{Q}(t) = \begin{bmatrix} \cos t & -\sin t \\ \sin t & \cos t \end{bmatrix}.$$

This transformation gives rise to the equation

$$\dot{\theta} = -\frac{i}{\hbar} \mathbf{E} \theta + \mathbf{A} \theta,$$

with

$$\mathbf{E} := \begin{bmatrix} 1 & 0 \\ 0 & -1 \end{bmatrix}$$

and

$$\mathbf{A} := \begin{bmatrix} 0 & -1 \\ 1 & 0 \end{bmatrix}.$$

Provided $\hbar \ll 1$, this system satisfies the quantum adiabatic theorem, which implies that the populations $\{|\theta_i(t)|^2\}$ are almost constant.

An exponential integrator for the system (31) is given by

$$\begin{aligned}\psi_{n+1} &= \exp\left(-\frac{i\Delta t}{2\hbar}\mathbf{H}_{n+1}\right)\exp\left(-\frac{i\Delta t}{2\hbar}\mathbf{H}_n\right)\psi_n \\ &= \mathbf{Q}_{n+1}^T \exp\left(-\frac{i\Delta t}{2\hbar}\mathbf{E}\right)\mathbf{Q}_{n+1}\mathbf{Q}_n^T \exp\left(-\frac{i\Delta t}{2\hbar}\mathbf{E}\right)\mathbf{Q}_n\psi_n\end{aligned}$$

or, in terms of θ , as

$$\theta_{n+1} = \exp\left(-\frac{i\Delta t}{2\hbar}\mathbf{E}\right)\mathbf{Q}_{n+1}\mathbf{Q}_n^T \exp\left(-\frac{i\Delta t}{2\hbar}\mathbf{E}\right)\theta_n. \quad (32)$$

Let us assume that the step size Δt is (accidentally) chosen such that

$$\exp\left(-\frac{i\Delta t}{2\hbar}\mathbf{E}\right) = \mathbf{I};$$

then (32) “simplifies” to

$$\theta_{n+1} = \mathbf{Q}_{n+1}\mathbf{Q}_n^T\theta_n,$$

which is a second-order-accurate discretization of the differential equation

$$\dot{\theta} = \mathbf{A}\theta = \dot{\mathbf{Q}}(t)\mathbf{Q}(t)^T\theta.$$

But this is wrong. The populations $\{|\theta_i(t)|^2\}$ are no longer conserved but undergo a systematic drift instead.

We point out that this effect is due to an unfortunate choice of the step size Δt and may not be observed generally. Nevertheless, it raises concerns about using a large time step when integrating a slowly varying time-dependent Schrödinger equation.

Provided that we can neglect the problem mentioned in Example 4, a larger macro step size Δt may be applied in (28)–(30), if the Born–Oppenheimer approximation (14) to the Hellmann–Feynman force is used in (29). See [8] for details. However, the formula (14) requires the computation of the derivatives of the diagonalized quantum operator $\mathbf{E}(\mathbf{q})$, which is computational expensive, in general. This can be avoided if an explicit averaging along $\psi(t)$ is applied to the Hellmann–Feynman force in (29). See [24] for details.

Here we suggest a different approach based on a splitting of the Hamiltonian (6) into $\mathcal{H} = \mathcal{H}_1 + \mathcal{H}_2$ in the following way [31]:

$$\mathcal{H}_1 = \frac{\mathbf{p}^T\mathbf{M}^{-1}\mathbf{p}}{2} \quad \text{and} \quad \mathcal{H}_2 = \langle\psi, \mathbf{H}(\mathbf{q})\psi\rangle + U(\mathbf{q}).$$

Let us write the corresponding differential equations. First, for \mathcal{H}_1 ,

$$\begin{aligned}\dot{\psi} &= \mathbf{0}, \\ \dot{\mathbf{q}} &= \mathbf{M}^{-1}\mathbf{p}, \\ \dot{\mathbf{p}} &= \mathbf{0};\end{aligned}$$

next, for \mathcal{H}_2 ,

$$\dot{\psi} = -\frac{i}{\hbar}\mathbf{H}(\mathbf{q})\psi, \quad (33)$$

$$\dot{\mathbf{q}} = \mathbf{0}, \quad (34)$$

$$\dot{\mathbf{p}} = -\langle \psi, \nabla_{\mathbf{q}}\mathbf{H}(\mathbf{q})\psi \rangle - \nabla_{\mathbf{q}}U(\mathbf{q}). \quad (35)$$

The solution to \mathcal{H}_1 is just a translation of classical particles with constant momentum \mathbf{p} .

The intriguing point about the second set of equations is that \mathbf{q} is now kept constant. Thus the vector ψ evolves according to a time-independent Schrödinger equation with constant Hamiltonian operator $\mathbf{H}(\mathbf{q})$, and the update of the classical momentum \mathbf{p} is obtained by integrating the Hellmann–Feynman forces [12] acting on the classical particles along the computed $\psi(t)$ (plus a constant update due to the purely classical force field).

Upon computing the eigenvalues of the operator $\mathbf{H}(\mathbf{q})$, Eqs. (33)–(35) can be solved exactly. However, this is, in general, an expensive undertaking. Therefore we proceed with the following multiple-time-stepping approach: The first step is to consider the identity

$$\exp(\Delta t L_{\mathcal{H}_2}) = \exp(\Delta t L_{\hat{\mathcal{H}}_2}) \cdot \exp(\Delta t L_U) = \underbrace{\exp(\delta t L_{\hat{\mathcal{H}}_2})}_{j \text{ times}} \cdot \exp(\Delta t L_U),$$

where $\delta t = \Delta t/j$, $j \gg 1$, and

$$\hat{\mathcal{H}}_2 = \langle \psi, \mathbf{H}(\mathbf{q})\psi \rangle.$$

The second step is to use

$$\exp(\Delta t L_{\mathcal{H}_1}) = \exp\left(\frac{\Delta t}{2} L_{\mathcal{H}_1}\right) \cdot \underbrace{\exp(\delta t L_{\hat{\mathcal{H}}_2})}_{j \text{ times}} \cdot \exp(\Delta t L_U) \cdot \exp\left(\frac{\Delta t}{2} L_{\mathcal{H}_1}\right) + \mathcal{O}(\Delta t^3). \quad (36)$$

The last step is to find a symplectic, second-order approximation $\Phi_{\delta t}$ to $\exp(\delta t L_{\hat{\mathcal{H}}_2})$. In principle, we can use any symplectic integrator suitable for time-dependent Schrödinger equations with a time-independent Hamilton operator $\mathbf{H}(\mathbf{q})$ (see, for example, [22]).

Provided that $\mathbf{V}(\mathbf{q})$ is diagonal, an efficient method $\Phi_{\delta t}$ is obtained by exploiting the natural splitting of the quantum operator $\mathbf{H}(\mathbf{q}) = \mathbf{T} + \mathbf{V}(\mathbf{q})$ as used in the symplectic PICKABACK scheme [29]. This yields two exactly solvable subsystems,

$$\hat{\mathcal{H}}_{2,1} = \langle \psi, \mathbf{T}\psi \rangle \quad \text{and} \quad \hat{\mathcal{H}}_{2,2} = \langle \psi, \mathbf{V}(\mathbf{q})\psi \rangle.$$

The resulting integrator for QCMD, as presented in Fig. 5 and first suggested in [31], is of second order, explicit, and symplectic, and conserves the norm of the wave function. For the implementation of other choices for $\Phi_{\delta t}$, see [31].

The MTS scheme of Fig. 5 may still require a relatively small macro step size Δt to ensure an accurate computation of the populations $\{|\theta_i(t)|^2\}$. Thus it might be useful to

Step 1.

$$\begin{aligned} \mathbf{q}_{n+1/2} &= \mathbf{q}_n + \frac{\Delta t}{2} \mathbf{M}^{-1} \mathbf{p}_n, \\ \hat{\mathbf{p}}_n &= \mathbf{p}_n - \Delta t \nabla_{\mathbf{q}} U(\mathbf{q}_{n+1/2}) \end{aligned}$$

Step 2.

$$k = 1 \dots j \quad \left\{ \begin{aligned} \hat{\psi}_{n+k/j} &= \exp\left(-\frac{i}{\hbar} \frac{\delta t}{2} \mathbf{T}\right) \psi_{n+(k-1)/j}, \\ \hat{\mathbf{p}}_{n+k/j} &= \hat{\mathbf{p}}_{n+(k-1)/j} - \delta t \langle \hat{\psi}_{n+k/j}, \nabla_{\mathbf{q}} \mathbf{V}(\mathbf{q}_{n+1/2}) \hat{\psi}_{n+k/j} \rangle, \\ \psi_{n+k/j} &= \exp\left(-\frac{i}{\hbar} \frac{\delta t}{2} \mathbf{T}\right) \exp\left(-\frac{i}{\hbar} \delta t \mathbf{V}(\mathbf{q}_{n+1/2})\right) \hat{\psi}_{n+k/j} \end{aligned} \right.$$

Step 3.

$$\begin{aligned} \mathbf{p}_{n+1} &= \hat{\mathbf{p}}_{n+1}, \\ \mathbf{q}_{n+1} &= \mathbf{q}_{n+1/2} + \frac{\Delta t}{2} \mathbf{M}^{-1} \mathbf{p}_{n+1}. \end{aligned}$$

FIG. 5. Multiple time stepping for QCMD.

consider the following modification of the MTS scheme (36):

$$\exp\left(\frac{\Delta t}{2} L_U\right) \cdot \underbrace{\left[\exp\left(\frac{\delta t}{2} L_{\mathcal{H}_1}\right) \cdot \exp(\delta t L_{\mathcal{H}_2}) \cdot \exp\left(\frac{\delta t}{2} L_{\mathcal{H}_1}\right) \right]}_{j \text{ times}} \cdot \exp\left(\frac{\Delta t}{2} L_U\right). \quad (37)$$

This MTS method resolves the quantum part of the QCMD equations of motion more accurately than (36) and is approximately as expensive as (36) if the evaluation of the operator $\mathbf{V}(\mathbf{q})$ and its gradient $\nabla_{\mathbf{q}} \mathbf{V}(\mathbf{q})$ is not too expensive compared to one integration step with $\Phi_{\delta t} \approx \exp(\delta t L_{\mathcal{H}_2})$.

EXAMPLE 2 (Continued). Here we numerically integrate the model system from Example 2 in Section 3.2. We use the symplectic and unitary implicit midpoint rule [40] for the numerical approximation of $\exp(\delta t L_{\mathcal{H}_2})$ and implement it in the MTS method (37). The Plank constant \hbar is set of $\hbar = 0.01$, the macro step size is $\Delta t = 0.1$, and $\delta t = 1.0 \times 10^{-3}$. As initial conditions, we take $q = 1$, $p = 0$, and $\psi = (1, 0)^T$. In Fig. 6, we plot the occupation numbers $|\theta_i(t)|^2$, $i = 1, 2$ and the time evolution of the classical coordinate $q(t)$. It can be seen that the Born–Oppenheimer approximation breaks down near $q(t) = 0.5$. Next we compare the “exact” solution obtained from the MTS method (37) with $\Delta t = 0.05$ and $\delta t = 1.0 \times 10^{-4}$ to the approximation obtained using the Verlet-based scheme (28)–(30) with a step size $\Delta t = 0.05$. The results can be found in Fig. 7. The difference in the trajectories is due to a (wrong) pointwise evaluation of the Hellmann–Feynman forces at a macro time step Δt in (29).

In summary, one can say that the design of MTS schemes for the QCMD model will require further research on an “optimal” choice for the method $\Phi_{\delta t}$ to approximate $\exp(\delta t L_{\mathcal{H}_2})$, the splitting of the Hamiltonian (6), and the ratio of the step sizes Δt and δt . Provided the eigendecomposition of the Hamilton operator $\mathbf{H}(\mathbf{q})$ is known, one could also directly

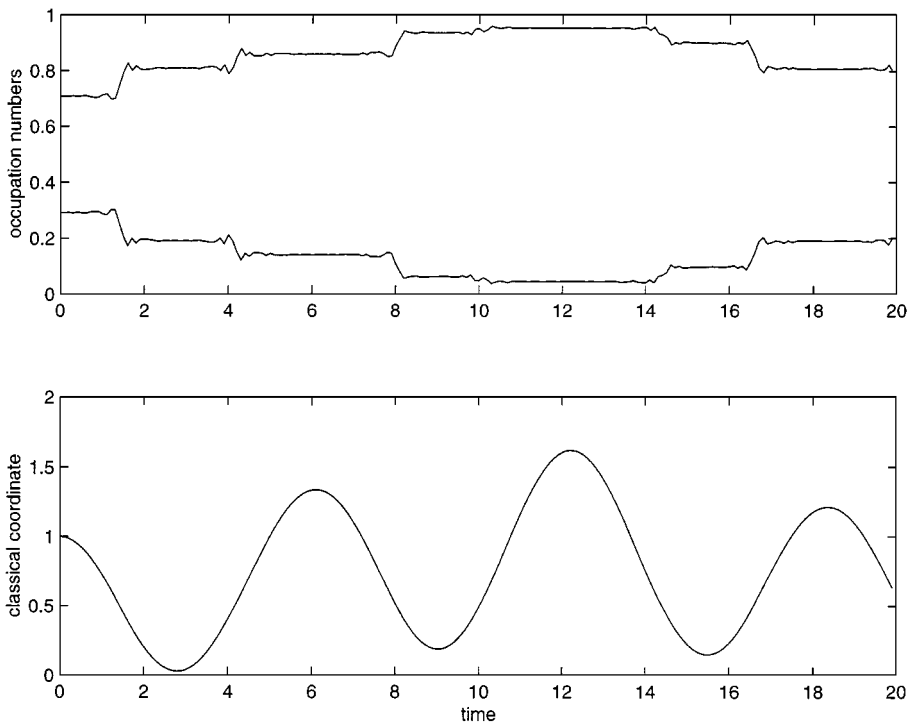


FIG. 6. Time evolution of the “occupation numbers” $|\theta_i(t)|^2$, $i = 1, 2$, and of the classical coordinate $q(t)$ over a time interval $[0, 20]$ using the symplectic MTS method (37).

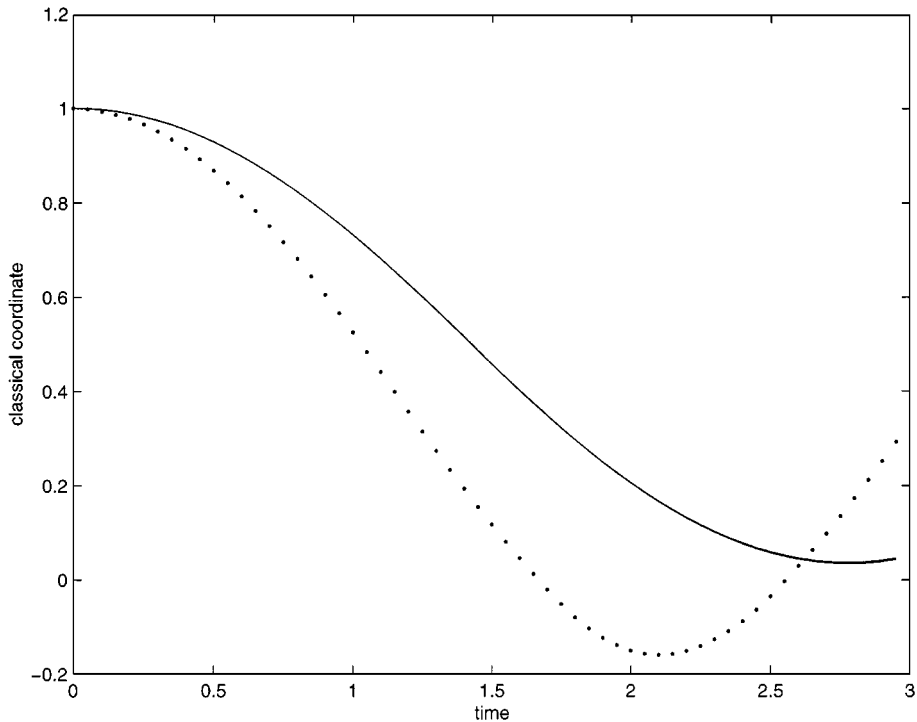


FIG. 7. Time evolution of the classical coordinate $q(t)$ computed with (i) the MTS method (37) (solid line) and (ii) the method (28)–(30) (dotted line).

integrate the transformed QCMD equations (9)–(11). This approach will be discussed in more detail in a forthcoming publication.

ACKNOWLEDGMENT

This work was started while the author was at the Konrad Zuse Center Berlin.

REFERENCES

1. M. P. Allen and D. J. Tildesley, *Computer Simulations of Liquids* (Clarendon Press, Oxford, 1987).
2. H. C. Anderson, Rattle: A ‘velocity’ version of the shake algorithm for molecular dynamics calculations, *J. Comput. Phys.* **52**, 24 (1983).
3. A. I. Arnold, *Mathematical Methods of Classical Mechanics* (Springer-Verlag, Berlin/New York, 1978).
4. U. Ascher and S. Reich, The midpoint scheme and variants for Hamiltonian systems: Advantages and pitfalls, *SIAM J. Sci. Comput.*, to appear.
5. G. Benettin, L. Galgani, and A. Giorgilli, Realization of holonomic constraints and freezing of high frequency degrees of freedom in the light of classical perturbation theory, II, *Commun. Math. Phys.* **113**, 557 (1989).
6. H. J. C. Berendsen and J. Mavri, Quantum simulation of reaction dynamics by density matrix evolution, *J. Phys. Chem.* **97**, 13464 (1993).
7. J. J. Biesiadecki and R. D. Skeel, Dangers of multiple-time-step methods, *J. Comput. Phys.* **109**, 318 (1993).
8. S. R. Billeter and W. F. van Gunsteren, A modular molecular dynamics/quantum dynamics program for nonadiabatic proton transfers in solution, *Comput. Phys. Commun.* **107**, 61 (1997).
9. T. Bishop, R. D. Skeel, and K. Schulten, Difficulties with multiple timestepping and the fast multipole algorithm in molecular dynamics, *J. Comput. Chem.* **18**, 1785 (1997).
10. M. Born and V. Fock, Beweis des Adiabatsatzes, *Z. Phys.* **51**, 165 (1928).
11. F. A. Bornemann, *Homogenization in Time of Singularly Perturbed Conservative Mechanical Systems*, Lecture Notes in Mathematics (Springer-Verlag, Berlin/New York, 1998), Vol. 1687.
12. F. A. Bornemann, P. Nettesheim, and Ch. Schütte, Quantum–classical molecular dynamics as an approximation for full quantum dynamics, *J. Chem. Phys.* **105**, 1074 (1996).
13. F. A. Bornemann and Ch. Schütte, On the singular limit of the quantum–classical molecular dynamics model, *SIAM J. Appl. Math.*, to appear.
14. F. Bornemann and Ch. Schütte, Homogenization of Hamiltonian systems with a strong constraining potential, *Physica D* **102**, 57 (1997).
15. F. Bornemann and Ch. Schütte, Approximation properties and limits of the quantum–classical molecular dynamics model, in *Computational Molecular Dynamics: Challenges, Methods, Ideas*, edited by P. Deuffhard et al., Lect. Notes in Comput. Sci. Eng. (Springer-Verlag, Berlin/New York, 1999), Vol. 4, p. 380.
16. J. M. Combes. The Born–Oppenheimer approximation, *Acta Phys. Austriaca* **17**, 139 (1977).
17. W. Dittrich and M. Reuter, *Classical and Quantum Dynamics* (Springer-Verlag, Berlin/New York, 1994), 2nd ed.
18. M. Fixman, Classical statistical mechanics of constraints: A theorem and application to polymers, *Proc. Natl. Acad. Sci.* **71**, 2635 (1974).
19. B. García-Archilla, J. M. Sanz-Serna, and R. D. Skeel, Long-time-step methods for oscillatory differential equations, *SIAM J. Sci. Comput.*, to appear.
20. A. García-Vela, R. B. Gerber, and D. G. Imre, Mixed quantum wave packet/classical trajectory treatment of the photodissociation process $\text{ArHCl} \rightarrow \text{Ar} + \text{H} + \text{Cl}$, *J. Chem. Phys.* **97**, 7242 (1992).
21. R. B. Gerber, V. Buch, and M. A. Ratner, Time-dependent self-consistent field approximation for intramolecular energy transfer, *J. Chem. Phys.* **66**, 3022 (1982).
22. S. K. Gray and D. E. Manolopoulos, Symplectic integrators tailored to the time-dependent Schrödinger equation, *J. Chem. Phys.* **104**, 7099 (1996).

23. H. Grubmüller, H. Heller, A. Windemuth, and K. Schulten, Generalized Verlet algorithm for efficient molecular dynamics simulations with long-range interactions, *Mol. Simul.* **6**, 121 (1991).
24. M. Hochbruck and Ch. Lubich, A bunch of time integrators for quantum/classical molecular dynamics, in *Computational Molecular Dynamics: Challenges, Methods, Ideas*, edited by P. Deuffhard *et al.*, Lect. Notes in Comput. Sci. Eng. (Springer-Verlag, Berlin/New York, 1999), Vol. 4, p. 421.
25. E. Helfand, Flexible vs. rigid constraints in statistical mechanics, *J. Chem. Phys.* **71**, 5000 (1979).
26. J. A. Izaguirre, S. Reich, and R. D. Skeel, Longer time steps for molecular dynamics, *J. Chem. Phys.*, to appear.
27. B. Leimkuhler and R. D. Skeel, Symplectic numerical integrators in constrained Hamiltonian systems, *J. Comput. Phys.* **112**, 117 (1994).
28. M. Mandziuk and T. Schlick, Resonance in the dynamics of chemical systems simulated by the implicit midpoint scheme, *Chem. Phys. Lett.* **237**, 525 (1995).
29. P. Nettesheim, F. A. Bornemann, B. Schmidt, and Ch. Schütte, An explicit and symplectic integrator for quantum–classical molecular dynamics. *Chem. Phys. Lett.* **256**, 581 (1996).
30. P. Nettesheim and Ch. Schütte, Numerical integrators for quantum–classical molecular dynamics, in *Computational Molecular Dynamics: Challenges, Methods, Ideas*, edited by P. Deuffhard *et al.*, Lect. Notes in Comput. Sci. Eng. (Springer-Verlag, Berlin/New York, 1999), Vol. 4, p. 396.
31. P. Nettesheim and S. Reich, Symplectic multiple-time-stepping integrators for quantum–classical molecular dynamics, in *Computational Molecular Dynamics: Challenges, Methods, Ideas*, edited by P. Deuffhard *et al.*, Lect. Notes in Comput. Sci. Eng. (Springer-Verlag, Berlin/New York, 1999), Vol. 4, p. 412.
32. S. Reich, Smoothed dynamics of highly oscillatory Hamiltonian systems, *Physica D* **89**, 28 (1995).
33. S. Reich, Torsion dynamics of molecular systems, *Phys. Rev. E* **53**, 4176 (1996).
34. S. Reich, *Dynamical Systems, Numerical Integration, and Exponentially Small Estimates* (Habilitationsschrift, Freie Universität Berlin, 1998).
35. S. Reich, A modified force field for constrained molecular dynamics, *Numer. Algorithms* **19**, 213 (1998).
36. H. Rubin and P. Ungar, Motion under a strong constraining force, *Comm. Pure Appl. Math.* **10**, 65 (1957).
37. J. P. Ryckaert, G. Ciccoliti, and H. J. C. Berendsen, Numerical integration of the Cartesian equations of motion of a system with constraints: Molecular dynamics of *n*-alkanes, *J. Comput. Phys.* **23**, 327 (1977).
38. U. Schmitt and J. Brinkmann, Discrete time-reversible propagation scheme for mixed quantum classical dynamics, *Chem. Phys.* **208**, 45 (1996).
39. U. Schmitt, *Gemischt klassisch-quantenmechanische Molekulardynamik im Liouville-Formalismus*, Ph.D. thesis, Darmstadt, 1997. [in German]
40. J. M. Sanz-Serna and M. P. Calvo, *Numerical Hamiltonian Systems* (Chapman and Hall, London, 1994).
41. F. Takens, Motion under the influence of a strong constraining force, in *Global Theory of Dynamical Systems*, Lecture Notes in Mathematics (Springer-Verlag, Berlin/New York, 1980), Vol. 819, p. 425.
42. M. Tuckerman, B. J. Berne, and G. J. Martyna, Reversible multiple time scale molecular dynamics, *J. Chem. Phys.* **97**, 1990 (1992).
43. L. Verlet, Computer experiments on classical fluids. I. Thermodynamical properties of Lennard–Jones molecules, *Phys. Rev.* **159**, 1029 (1967).
44. J. Zhou, S. Reich, and B. R. Brooks, Elastic molecular dynamics with flexible constraints, submitted for publication.